Bandwidth Enhancement by Master Modulation of Optical Injection-Locked Lasers

Erwin K. Lau, *Member, IEEE, Member, OSA*, Liang Jie Wong, Xiaoxue Zhao, *Member, IEEE*, Young-Kai Chen, *Fellow, IEEE*, Connie J. Chang-Hasnain, *Fellow, IEEE, Fellow, OSA*, and Ming C. Wu, *Fellow, IEEE, Member, OSA*

***Abstract*—In normal injection-locked semiconductor lasers, the modulation signals are applied to the slave laser. In this paper, we show that modulating the master light before injection exhibits distinctive modulation dynamics and frequency response. We first present a detailed theoretical model and simulation results. Experimentally, we have successfully demonstrated both master amplitude and master phase modulation. The resulting 3-dB bandwidths have been enhanced by up to three times, exceeding 50 GHz. The resonance frequency of the combined lasers is greater than 100 GHz.**

***Index Terms*—Injection locking, modulation frequency response, semiconductor lasers.**

I. Introduction

THE growing need for larger transmission speeds in optical communications has driven much research in developing higher bandwidth modulation schemes. The most venerable of these techniques, direct modulation of a semiconductor laser, is cost-effective and simple, but practical limitations, including heating and gain compression [1], have restricted 3-dB bandwidths $(f_{3\mathrm{dB}})$ to 30–40 GHz [2]–[4]. External modulation techniques, which are not limited by laser dynamics, have demonstrated bandwidths $>$100 GHz for electrooptic modulators (EOMs) [5] and $>$50 GHz for electroabsorption modulators (EAMs) [6]. However, velocity and impedance mismatches and material losses ultimately limit the bandwidth of these devices. As the practical limitations to the bandwidth for these devices are reached, other techniques must be developed to further increase modulation bandwidths for next-generation optical systems.

Optical injection-locked (OIL) lasers hold promise as a technique that can surpass these limitations. Optical injection locking has been shown to increase the resonance frequency and bandwidth of the direct-modulated laser [7]–[9]. Previously, we have demonstrated resonance frequencies up to 107 GHz and intrinsic bandwidths up to 80 GHz [10]. The modulated laser is a relatively short-gain device and therefore does not suffer from velocity mismatches or material loss issues. Resistance–capacitance (*RC*) parasitics can also be minimized by proper design.

However, in the injection-locked laser, the resonance frequency does not necessarily determine the bandwidth, as it does for the free-running, direct-modulated laser. The OIL laser, in specific circumstances, can experience a low-frequency pole that can severely limit its response [10], [11]. This pole is independent from the *RC* parasitics inherent in the laser packaging and can be derived from the laser dynamics. The effects of this low-frequency pole can be mitigated in two ways. The first is by enhancement of the pole frequency by increasing the bias current of the slave laser [10] or increasing the linewidth enhancement factor [11], [12]. The second method is by cancellation of the pole via modulation of the master laser. This latter method is the topic of this paper.

Previously, we have demonstrated the method of bandwidth enhancement by modulating the master laser of an OIL system [13]. We have experimentally shown master amplitude modulated (MAM) as well as master phase modulated (MPM) OIL systems. Several works in the past have performed master modulation of injection-locked lasers. However, they focus on applications of amplitude modulation suppression that require low-injection regimes [14]–[21] or FM discrimination [22]. Here, we focus on enhancement of the modulation bandwidth of a modulator by either amplitude modulation (AM) or phase modulation (PM) amplification. The concept is shown schematically in Fig. 1. In this example, the modulator whose bandwidth will be enhanced is a phase modulator with a 3-dB bandwidth of 60 GHz. The master laser, before injection, is first modulated by a phase modulator (simulation shown in left response graph). The modulated light is then injected into the slave laser. The dc power of the master laser locks the slave laser, creating a resonance peak at the enhanced frequency identical to the one analyzed in the direct modulation OIL case [11]. The resonance is tuned to three times the modulator bandwidth (middle response graph). The injected phase modulation near the resonance is thus enhanced, broadening the final PM bandwidth to 3.3 times the modulator bandwidth (right response graph). This would result in a bandwidth of 200 GHz, much larger than the 60-GHz limitation of the PM by itself. This technique does not suffer from the low-frequency roll-off that limits direct-modulated OIL systems. Furthermore, the enhancement is relative to the bandwidth of the original modulator and can be up to 3.7 times for an ideal single-pole modulator. Our simulations show that a

Manuscript received January 29, 2008; revised May 27, 2008. Current version published October 10, 2008. This work was supported in part by the DARPA aPROPOS program under Contract W911NF-06-1-0269 (S. Pappert) and the DARPA seedling program on high-speed lasers under Contract W911NF-07-1-0468 (H. Temkin).

E. K. Lau, L. J. Wong, X. Zhao, C. J. Chang-Hasnain, and M. C. Wu are with the Department of Electrical Engineering and Computer Sciences, University of California, Berkeley, CA 94720 USA (e-mail: elau@eecs.berkeley.edu).

Y.-K. Chen is with Bell Laboratories, Alcatel-Lucent, Murray Hill, NJ 07974 USA (e-mail: ykchen@alcatel-lucent.com).

Color versions of one or more of the figures in this paper are available online at http://ieeexplore.ieee.org.

Digital Object Identifier 10.1109/JLT.2008.927192

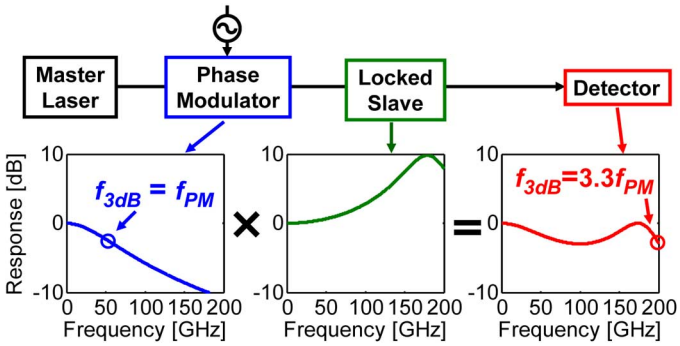

Fig. 1. Conceptual diagram of bandwidth enhancement by master modulation. The example shown is for master phase modulation.

100-GHz modulator can be enhanced up to 370 GHz by setting the resonance to 316 GHz. We have already shown that injection locking can achieve resonance frequencies >100 GHz [10], with promise of higher frequencies in the near future. The technique can also be used to resonantly enhance master AM as well. In this case, the master light is amplitude-modulated, and the resonance peak will enhance the AM bandwidth, resulting in a broader bandwidth AM response. Although, in this example and the subsequent experimental demonstrations in this paper, we use external modulators, these are used only for proof-of-concept. The original modulation source may be from any modulator: either EOM, EAM, integrated electroabsorption modulation laser (EML), or direct-modulated (DM) master laser. With the prospect of viable integrated optical isolators [23], full integration of all components of a monolithic injection locked laser system onto one chip promise to make cost-effective, ultrahigh bandwidth modulators possible.

In this paper, we first present a theoretical analysis of the master modulation OIL technique and describe how to bias the laser to achieve maximum bandwidth enhancement. We then experimentally enhance the 3-dB bandwidth of an amplitude-modulated optical signal and a phase-modulated optical signal, demonstrating the technique's versatility. Utilizing these techniques, we demonstrate bandwidths of >59 GHz for MAM-OIL and 53 GHz for MPM-OIL. In addition, we show that the system can be dynamically tuned to enhance frequency bandwidths centered on resonances >100 GHz.

II. Theory

To analyze the frequency response of the injection-locked laser, we perform a small-signal analysis on the commonly-used injection-locked laser rate equations [24]–[27]. Laser parameters for all simulations are listed in [11], except $J = 1.5 \times J_{\rm th}$ was used. The differential equation governing the complex field of an injection-locked laser is similar to that of a free-running laser, with the addition of an injection term

$$\frac{dE(t)}{dt} = \frac{1}{2}g[N(t) - N_{\rm th}](1 + j\alpha)E(t) + \kappa E_{\rm inj}(t) - j\Delta\omega_{\rm inj}E(t) \quad (1)$$

where $E(t)$ is the slave laser's complex field and $E_{\rm inj}(t)$ is the injected master field. Here, we add time dependence to the injected field to accommodate modulation of the master light. This model ignores contributions from spontaneous emission, gain compression and noise, but may easily be modified to include these effects. This equation can be split into the field magnitude and phase by assuming that $E(t) = \sqrt{S(t)}\exp[j\phi(t)]$, where $S(t)$ is the slave laser's internal photon number and $\phi(t)$ is the slave laser phase, relative to the nominal master phase. Similarly, the injection term may be split into $E_{\rm inj}(t) = \sqrt{S_{\rm inj}(t)}\exp[j\phi_{\rm inj}(t)]$, where $S_{\rm inj}(t)$ is the injected master laser photon number and $\phi_{\rm inj}(t)$ is the time-dependent master laser phase. The split equations, along with the carrier rate equation, constitute the three differential equations of injection-locked lasers [11], [14], [28]:

$$\frac{dS(t)}{dt} = g[N(t) - N_{\rm th}]S(t) + 2\kappa\sqrt{S_{\rm inj}(t)S(t)}\cos[\phi(t) - \phi_{\rm inj}(t)] \quad (2)$$

$$\frac{d\phi(t)}{dt} = \frac{\alpha}{2}g[N(t) - N_{\rm th}] - \kappa\sqrt{\frac{S_{\rm inj}(t)}{S(t)}}\sin[\phi(t) - \phi_{\rm inj}(t)] - \Delta\omega_{\rm inj} \quad (3)$$

$$\frac{dN(t)}{dt} = J(t) - \gamma_N N(t) - \{\gamma_p + g[N(t) - N_{\rm th}]\}S(t) \quad (4)$$

where $N(t)$ is the slave laser's carrier number. $\Delta\phi = \phi(t) - \phi_{\rm inj}(t)$ is the phase difference between master and slave. $g, N_{\rm th}, \alpha, J, \gamma_N$, and γ_P are the slave laser's linear gain coefficient, threshold carrier number, linewidth enhancement factor, bias current, carrier recombination rate, and photon decay rate, respectively. The injection terms, κ and $\Delta\omega_{\rm inj}$ are the coupling rate [29] and detuning frequency, respectively. The detuning frequency is defined as the difference between master laser and free-running slave laser frequency: $\Delta\omega_{\rm inj} = \omega_{\rm master} - \omega_{\rm slave,fr}$. Here, we use photon number (S), in contrast to field used in [11], to more directly relate to photon amplitude. For a sinusoidal, small-signal perturbation, each time-dependent term may be separated into its dc and sinusoidal parts:

$$\begin{aligned} J(t) &= J_0 + \Delta J\exp(st) \\ S_{\rm inj}(t) &= S_{inj0} + \Delta S_{\rm inj}\exp(st) \\ \phi_{\rm inj}(t) &= \phi_{inj0} + \Delta\phi_{\rm inj}\exp(st) \\ S(t) &= S_0 + \Delta S\exp(st) \\ \phi(t) &= \phi_0 + \Delta\phi\exp(st) \\ N(t) &= N_0 + \Delta N\exp(st) \end{aligned} \quad (5)$$

where the first terms on the right-hand-sides are the dc components and the ΔX (where X is $J, S_{\rm inj}, \phi_{\rm inj}, S, \phi$, or N) terms are the magnitude of the perturbation terms. The first three time-dependent terms ($J, S_{\rm inj}$, and $\phi_{\rm inj}$) may be considered the inputs to the system, while the last three terms (S, ϕ, and N) are the outputs. Physically, ΔJ represents direct modulation of the current, $\Delta S_{\rm inj}$ represents modulation of the amplitude of the injected light (MAM-OIL), and $\Delta\phi_{\rm inj}$ represents modulation of the phase of the injected light (MPM-OIL). The typical output of a direct-modulated laser is ΔS, which represents the modulated amplitude of the slave. In MAM-OIL, we consider this as the output as well. Here, we consider the modulated phase of

the slave, $\Delta\phi$, as an output for the MPM-OIL technique. The input perturbation terms ($\Delta J, \Delta S_{\rm inj}$, and $\Delta\phi_{\rm inj}$) are typically excited separately, but may be excited simultaneously. A complex phasor may be added to represent a phase offset between driving terms. For this work, however, we will consider each driving term separately, so the driving perturbation magnitudes may be considered real phasors.

Without loss of generality, we may set the dc master phase to zero: $\phi_{\rm inj0} = 0$, so that the dc slave phase ϕ_0 represents the total dc phase difference between master and slave. Inserting (5) into (2)–(4), linearizing, and then separating the dc and sinusoidal perturbation parts yields the dc and small-signal solutions. The steady-state solutions, repeated here, are equivalent to those solved for a purely direct-modulated OIL case, and the derivation can be found in more detail in [11]:

$$S_0 = \frac{S_{\rm fr} - \frac{\gamma_N}{\gamma_P}\Delta N_0}{1 + \frac{g\Delta N_0}{\gamma_P}} \tag{6}$$

$$\phi_0 = \sin^{-1}\left\{-\frac{\Delta\omega_{\rm inj}}{\kappa\sqrt{1+\alpha^2}}\sqrt{\frac{S_0}{S_{\rm inj0}}}\right\} - \tan^{-1}\alpha \tag{7}$$

$$\Delta N_0 = -\frac{2\kappa}{g}\sqrt{\frac{S_{inj0}}{S_0}}\cos\phi_0 \tag{8}$$

where $\Delta N_0 \equiv N_0 - N_{\rm th}$ and the free-running photon number $S_{\rm fr}$ is

$$S_{\rm fr} = \frac{J - \gamma_N N_{\rm th}}{\gamma_P}. \tag{9}$$

The two important locking bias parameters are the detuning frequency $\Delta f = \Delta\omega_{\rm inj}/2\pi$ and the injection ratio $R = S_{\rm inj0}/S_{\rm fr}$.

A. Small-Signal Solutions

When linearized, the differential equations may be placed into matrix form

$$\begin{bmatrix} m_{\rm SS}+s & m_{S\phi} & m_{\rm SN} \\ m_{\phi S} & m_{\phi\phi}+s & m_{\phi N} \\ m_{\rm NS} & 0 & m_{\rm NN}+s \end{bmatrix}\begin{bmatrix}\Delta S\\ \Delta\phi\\ \Delta N\end{bmatrix} = \begin{bmatrix}0\\0\\1\end{bmatrix}\Delta J e^{j\theta_J} + \begin{bmatrix} z\cos\phi_0 S_0/S_{inj0} \\ -z\sin\phi_0/2S_{inj0} \\ 0\end{bmatrix}\Delta S_{\rm inj}e^{j\theta_{\rm Sinj}} + \begin{bmatrix}2zS_0\sin\phi_0\\ z\cos\phi_0\\0\end{bmatrix}\Delta\phi_{\rm inj}e^{j\theta_{\phi inj}} \tag{10}$$

where s is considered to be along the $j\omega$ axis. The elements of the transition matrix $\bar{M}$ are

$$\begin{aligned} m_{\rm SS} &= z\cos\phi_0 \\ m_{S\phi} &= 2zS_0\sin\phi_0 \\ m_{\rm SN} &= -gS_0 \\ m_{\phi S} &= -z\sin\phi_0/2S_0 \\ m_{\phi\phi} &= z\cos\phi_0 \\ m_{\phi N} &= -\frac{\alpha}{2}g \\ m_{\rm NS} &= \gamma_P - 2z\cos\phi_0 \\ m_{\rm NN} &= \gamma_N + gS_0 \end{aligned} \tag{11}$$

where $z \equiv \kappa\sqrt{S_{inj0}/S_0}$. The left-hand side represents the input terms and the transition matrix that links them to the driving terms. The right-hand side of the equation represents the three different driving perturbations. Complex phase terms $(\theta_J, \theta_{\rm Sinj}, \theta_{\phi\rm inj})$ were included to represent the general case where a phase offset between sinusoidal driving terms may exist. Again, since we will consider each driving term separately in this work, we set these terms to 0. The frequency response of the output perturbations may be found by inverting the transition matrix and solving for each separate driving term. For direct modulation, we obtain

$$\begin{bmatrix}\Delta S\\ \Delta\phi\\ \Delta N\end{bmatrix} = \bar{M}^{-1}\begin{bmatrix}0\\0\\1\end{bmatrix}\Delta J. \tag{12}$$

For master amplitude modulation

$$\begin{bmatrix}\Delta S\\ \Delta\phi\\ \Delta N\end{bmatrix} = \bar{M}^{-1}\begin{bmatrix} z\frac{S_0}{S_{inj0}}\cos\phi_0 \\ -z\frac{1}{2S_{inj0}}\sin\phi_0 \\ 0\end{bmatrix}\Delta S_{\rm inj}. \tag{13}$$

Finally, for master phase modulation

$$\begin{bmatrix}\Delta S\\ \Delta\phi\\ \Delta N\end{bmatrix} = \bar{M}^{-1}\begin{bmatrix}2zS_0\sin\phi_0\\ z\cos\phi_0\\0\end{bmatrix}\Delta\phi_{\rm inj}. \tag{14}$$

The important output terms will differ, depending on the purpose and source of modulation. For direct modulation, the output is typically photon modulation $\Delta S/\Delta J$:

$$H_{\rm DM} \equiv \frac{\Delta S}{\Delta J} = M_D\frac{s - Z_D}{s^3 + As^2 + Bs + C} = M_D\frac{s+\omega_{\rm ZD}}{D(s)} \tag{15}$$

where

$$\begin{aligned} A &= m_{\rm SS} + m_{\phi\phi} + m_{\rm NN} \\ B &= m_{\rm SS}m_{\phi\phi} + m_{\rm SS}m_{\rm NN} + m_{\phi\phi}m_{\rm NN} \\ &\quad - m_{S\phi}m_{\phi S} - m_{\rm SN}m_{\rm NS} \\ C &= m_{\rm SS}m_{\phi\phi}m_{\rm NN} + m_{S\phi}m_{\phi N}m_{\rm NS} \\ &\quad - m_{S\phi}m_{\phi S}m_{\rm NN} - m_{\rm SN}m_{\rm NS}m_{\phi\phi} \\ M_D &= -m_{\rm SN}. \end{aligned} \tag{16}$$

The zero $-\omega_{ZD}$ is real and larger than the resonance frequency:

$$\omega_{ZD} = (m_{SN}m_{\phi\phi} - m_{S\phi}m_{\phi N})/m_{\rm SN}. \tag{17}$$

It has little effect on the frequency response of the direct-modulated OIL laser for frequencies below the resonance.

Note that each modulation source shares the same determinant $D(s)$, which is composed of three poles:

$$D(s) = (s+\omega_P)\left(s - j\omega_R + \frac{1}{2}\gamma\right)\left(s + j\omega_R + \frac{1}{2}\gamma\right). \tag{18}$$

This implies that all modulation methods (direct modulation on slave laser, AM on master laser, and PM on master laser) share the same resonance frequency ω_R, damping γ, and low-

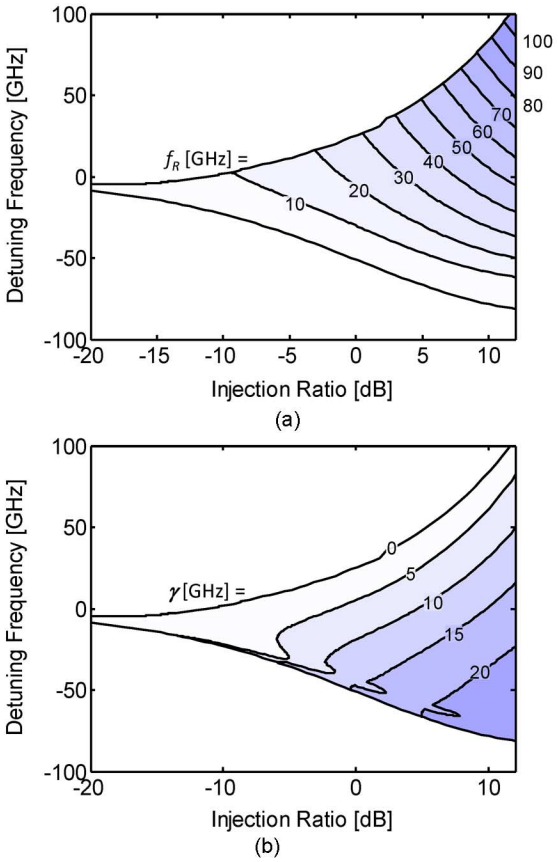

Fig. 2. Theoretical plot of (a) resonance frequency and (b) damping versus injection ratio and detuning frequency.

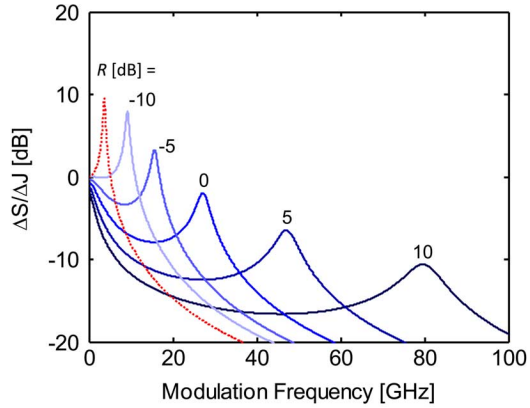

Fig. 3. Frequency response of direct-modulated OIL laser, for different injection ratios. Dotted red curve is the free-running response.

frequency roll-off pole ω_P as discussed in [11]. Hence, the resonance frequency should increase with both injection ratio and detuning frequency:

$$\omega_R^2 \approx \omega_{R0}^2 + \Delta\omega_R^2 \tag{19}$$

where ω_{R0} is the free-running resonance frequency and the resonance frequency enhancement term $\Delta\omega_R$ is

$$\Delta\omega_R = \left|\kappa\sqrt{\frac{S_{\text{inj0}}}{S_0}}\sin\phi_0\right| = \left|-\frac{\alpha}{2}g(N_0 - N_{\text{th}}) + \Delta\omega_{\text{inj}}\right|. \tag{20}$$

The resonance frequency is plotted across the locking range in Fig. 2, which clearly shows the resonance enhancement and damping for an OIL laser. However, as explained in [11], the low-frequency roll-off pole will dominate the 3-dB bandwidth at very high ω_R. This roll-off is shown in Fig. 3. As we increase the injection ratio and enhance ω_R, ω_P decreases and causes the 3-dB frequency to shrink rather than increase. A more extensive discussion on direct modulation OIL and methods for increasing the low-frequency roll-off pole is given in [11].

Equations (12)–(14) imply that, since all three modulation sources share the same poles, both master modulation techniques should also suffer from the same low-frequency roll-off that limits direct modulation. However, we will subsequently see that an additional low-frequency zero in the MAM-OIL and MPM-OIL modulation formats largely cancels the effect of the low-frequency pole at large resonance frequencies. In the following two sections, we will analyze the small-signal response of the two master modulation techniques.

B. Master Amplitude Modulation Optical Injection Locking

For master amplitude modulation, the input is an AM signal from an EOM, EML, direct-modulated laser, or any other amplitude modulator. We modulate the master light (ΔS_{inj}), injection-lock the slave, then detect the AM light from the slave. The MAM response is thus

$$H_{\text{MAM}} \equiv \frac{\Delta S}{\Delta S_{\text{inj}}} = M_A\frac{(s+\omega_{ZA1})(s+\omega_{ZA2})}{D(s)} \tag{21}$$

where

$$\begin{aligned}\omega_{ZA1} &= \frac{z}{\cos\phi_0}\\ \omega_{ZA2} &= \gamma_N + gS_0\\ M_A &= z\cos\phi_0\frac{S_0}{S_{\text{inj0}}}.\end{aligned} \tag{22}$$

Representative frequency response curves are shown in Fig. 4. $-\omega_{ZA1}$ and $-\omega_{ZA2}$ are both real and negative. However, ω_{ZA1} is larger than ω_R and tends to have little effect on the response's shape until beyond the resonance frequency. ω_{ZA2} is, on the other hand, much smaller than ω_R, being related to the enhanced carrier recombination rate from stimulated emission. If compared to ω_P, which is approximately (when the resonance frequency enhancement is significantly large)

$$\omega_P \approx \frac{C}{z^2} \approx \gamma_N + \left(1 + \frac{\alpha}{\tau_p\omega_R}\right)gS_0 \tag{23}$$

it is on the same order of magnitude, and they only differ by the last term in (23), which is typically positive. Since ω_{ZA2} is slightly smaller in magnitude than ω_P, it will cause a dip in response at dc, which is the origin of the AM suppression discussed in the previous literature [14]–[21]. From (21) and (22), the dc response is

$$H_{\text{MAM}}(j\omega = 0) = \frac{\kappa^2(\gamma_N + gS_0)}{C} \approx \frac{gS_0^2}{\omega_P S_{\text{inj0}}}. \tag{24}$$

Hence, to increase the dc response, ω_P would need to decrease. One would minimize α, decrease the detuning frequency, and

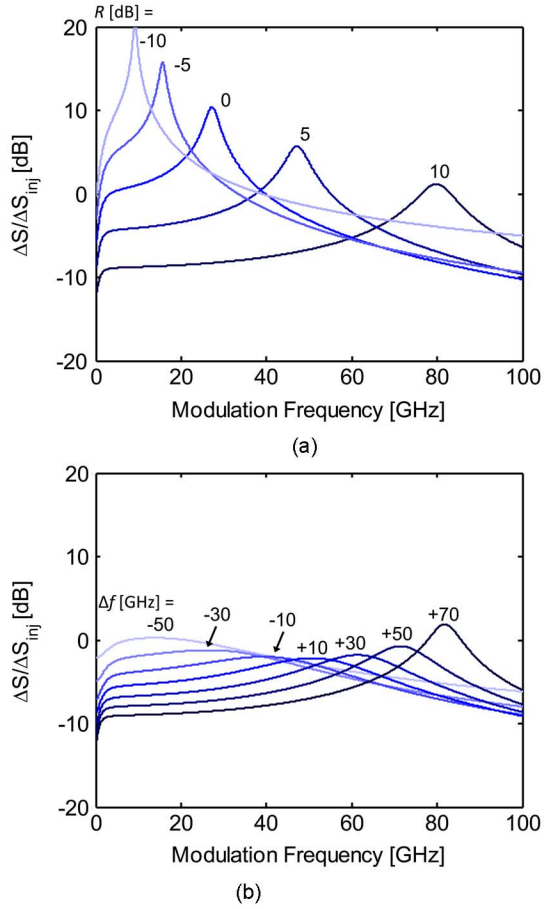

Fig. 4. Frequency response of master amplitude-modulated OIL laser, for (a) different injection ratios and (b) different detuning frequencies (R = 10 dB).

increase the slave laser bias. This can result in low-frequency gain. We can also approximate the response for positive detuning values where ω_P is significantly smaller than the resonance frequency. Here, sufficiently above the frequency of both the low-frequency pole ω_P and zero ω_{ZA2}, the response approximates to

$$H_{\mathrm{MAM}} \approx \frac{\kappa^2}{\omega_R^2 - \omega^2 + j\gamma\omega}. \tag{25}$$

Hence, the response approximates to a classic two-pole laser response above dc, as seen in the large frequency detuning cases ($\Delta f > +10$ GHz) in Fig. 4. If the response is taken at the flat region between dc and resonance, the response then approximates further to

$$H_{\mathrm{MAM}} \approx \frac{S_0}{S_{inj0}} \tag{26}$$

which signifies that gain can also occur for small injection ratios. However, small injection ratios result in low bandwidths and, hence, are not studied here.

To maximize the bandwidth, we tune the resonance frequency and damping such that the resonance will enhance the response of the original modulator at the point where it begins to drop, as conceptually done in Fig. 1. When optimized, the 3-dB bandwidth can be enhanced up to 3.3 times the original bandwidth, while keeping <3-dB ripple in the final response. At high injection ratios, the drop in dc response near the positive detuning edge is due to the drop in dc optical power from the injection level to the slave output level. This may be acceptable if the dc power must be maintained below a certain level, for example, so as not to saturate the photodetector.

C. Master Phase Modulation Optical Injection Locking

For master phase modulation, the input is a PM signal from a phase modulator, integrated or external. The output is the modulation response of the slave laser's phase. The MPM response is

$$\begin{aligned} H_{\mathrm{MPM}} &\equiv \frac{\Delta\phi}{\Delta\phi_{\mathrm{inj}}} = \frac{as^2 + bs + C}{D(s)} \\ &= M_P \frac{(s+\omega_{ZP1})(s+\omega_{ZP2})}{D(s)} \end{aligned} \tag{27}$$

where

$$\begin{aligned} \omega_{ZP1,2} &= (b \pm \sqrt{b^2 - 4aC})/2a \\ M_P &\equiv a \equiv z\cos\phi_0 \\ b &= z[z + \cos\phi_0(\gamma_N + gS_0)] \end{aligned} \tag{28}$$

where we assumed $gS_0 \gg \gamma_N$. Before analyzing the poles in (28), we first note that the first equality in (27), along with the definition of the determinant, D in (15), shows that as the modulation frequency goes to dc (i.e., $s \to j\omega = 0$), the magnitude of the MPM response equals C/C, and thus approaches unity. This is consistent with the view that the slave laser phase should track any changes in the master laser phase.

For strong injection, $z \gg gS_0$, then $b^2 \gg 4aC$ and the zeros can be approximated as

$$\begin{aligned} \omega_{ZP1} &\approx \frac{z}{\cos\phi_0} + gS_0 \\ \omega_{ZP2} &\approx \frac{C}{z^2}. \end{aligned} \tag{29}$$

ω_{ZP1} is typically larger than ω_{ZA1} and is therefore large enough not to affect the shape of the response until above the resonance frequency. The zero, ω_{ZP2}, is approximately equal to the pole, ω_P, and therefore cancel. Hence, the response

$$H_{\mathrm{MPM}} \approx \frac{\omega_R^2}{\omega_R^2 - \omega^2 + j\gamma\omega} \tag{30}$$

which resembles a damped oscillator with a resonance frequency of ω_R. Fig. 5 plots this response for various injection ratios and detuning frequencies. The phase-tracking bandwidth increases with injection power because the increased injection energy forces the slave to track the master phase more quickly. The response is not limited by the K-factor of free-running lasers, so the resonance frequency can be tuned extremely high. Since we can control both the resonance frequency and damping, we can create almost any response profile.

The cancellation of the low-frequency pole can be explained by Fig. 6, which depicts the dynamics of the carriers, photons and phase energy reservoirs. Panel (a) represents the direct-

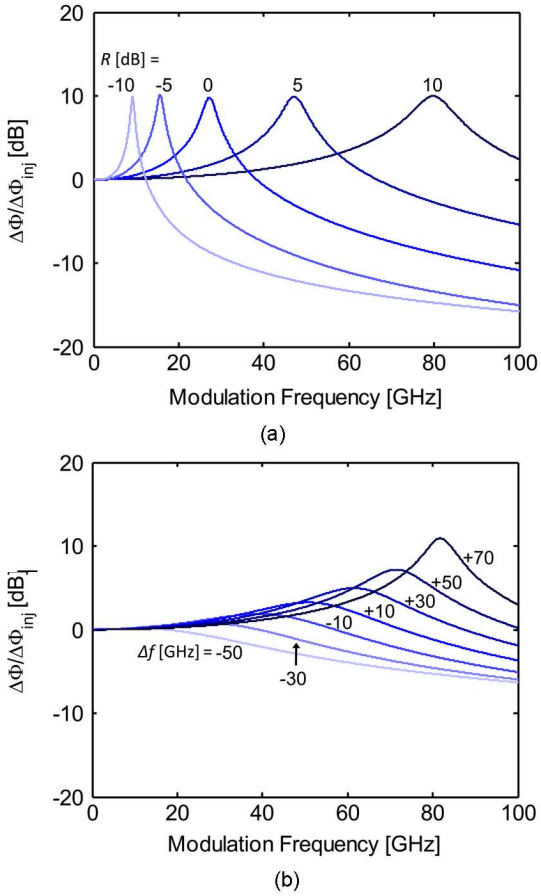

Fig. 5. Frequency response of master phase-modulated OIL laser, for (a) different injection ratio and (b) different detuning frequencies ($R = 10$ dB).

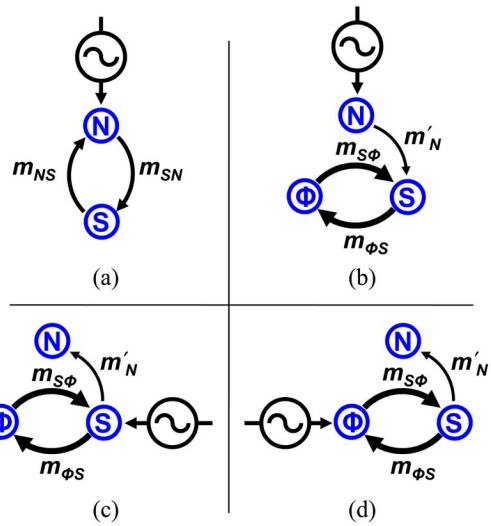

Fig. 6. Schematics of the carrier (N)/photon (S)/phase (ϕ) dynamics for (a) direct-modulated free-running laser, (b) direct-modulated OIL laser, (c) master amplitude-modulated OIL laser, and (d) master phase-modulated OIL laser.

modulated, free-running case. The resonance frequency is determined by the rates (arrows) of energy transfer between carriers and photons: $\omega_{\mathrm{RO}} = \sqrt{m_{\mathrm{NS}} m_{\mathrm{SN}}}$, which can typically range from 1–40 GHz. The modulation is applied to the carriers. Panel (b) represents the injection-locked, direct-modulated case. Here, the energy transfer between photons and the phase becomes dominant, and, for large R and $\Delta f, \omega_{\mathrm{RO}} \approx \sqrt{m_{\phi S} m_{S\phi}}$, which corresponds to the enhanced resonance frequency of injection-locked lasers. This has been shown to be enhanced >100 GHz [10]. Again, the modulation is applied to the carriers, but the carriers lie outside of the dominant dynamics (phase and photons). Hence, the speed of the laser is bottlenecked by the rate in which the carriers can transfer energy to the photons and phase. This is represented by the rate m'_N, which is dominated by the carrier recombination rate enhanced by stimulated emission. This can be as low as 1 GHz, but has been experimentally enhanced to >22 GHz [10]. This rate is proportional to ω_P, and typically determines the bandwidth of the laser [10], [11]. In reality, another rate enhances the rate of carrier energy in to the resonance. The circular coupling of carriers to phase to photons also enhances ω_P. This is not shown in Fig. 6. Panel (c) and (d) represent the injection-locked master-modulated case of AM and PM, respectively. In both these cases, the modulation is applied directly to the dominant resonance dynamics: photons in the MAM case and phase in the MPM case. Hence, the low-frequency pole is largely canceled, and the frequency response tends to resemble that of a classic two-pole laser response with a greatly enhanced resonance frequency.

III. Experiment

In this section, we experimentally demonstrate bandwidth enhancement for both amplitude and phase modulation schemes. The experimental setup for MAM-OIL and MPM-OIL is shown in Fig. 7(a) and (b), respectively. Here, the MAM is created by a zero-chirp, $LiNbO_3$ EOM. The MPM is created by a $LiNbO_3$ phase modulator. It is important to reiterate that the technique is not limited to the modulators used here and can be integrated with either master or slave. Both modulators were preceded by a high-power 1550-nm, single-mode, butterfly-packaged laser. Frequency detuning was accomplished by temperature tuning the master. Injection locking power was changed by either changing the EDFA output power or by a variable optical attenuator. Locking conditions were checked to assure stable locking in all cases. The slave laser is a 1550-nm distributed feedback laser. A polarization controller (PC) is used to optimize the input polarization to the $LiNbO_3$ modulators. The output of the modulators is amplified by an erbium-doped fiber amplifier (EDFA). Another PC is used to optimize the coupling polarization into the slave laser. An optical isolator is used to prevent optical feedback to the master laser. The master laser is injected into the slave by an optical coupling head with 3-dB insertion loss. The modulated slave laser light is coupled to another optical head on the opposing facet. It is then optically amplified and then detected. Electrical modulation and detection are performed by a vector network analyzer. Detection of the phase modulation was performed by the AM/PM separation technique described by Sorin *et al.* [30]. We used a 0.95-nm bandwidth tunable optical filter (Santec OTF-920) after the slave laser output to obtain frequency discrimination at both quadrature points of the filter.

The free-running frequency response of the slave laser, biased at 2.4 times threshold, is shown in Fig. 8 (labeled DM-FR).

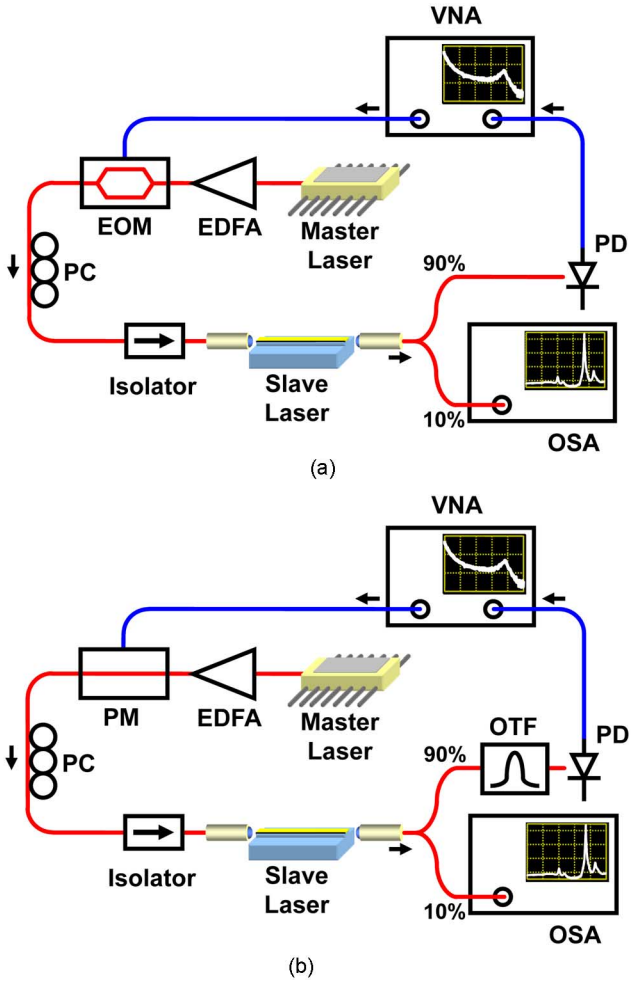

Fig. 7. Experimental setup for (a) MAM-OIL and (b) MPM-OIL. EDFA = erbium-doped fiber amplifier, EOM = electrooptic modulator, PC = polarization controller, PD = photodetector, VNA = vector network analyzer, OSA = optical spectrum analyzer, PM = phase modulator, and OTF = optical tunable filter.

Its resonance frequency (f_{RO}) is 3 GHz and its 3-dB bandwidth $(f_{3\mathrm{dB}})$ is 4 GHz. We then injection lock the slave laser. The injection ratio R (defined as the optical power ratio of the master and free-running slave, measured at the injected slave laser facet) was 3 dB. The detuning frequency Δf (defined as the frequency difference between master and free-running slave) was +12.4 GHz. These injection-locking conditions were kept constant for all examples in Fig. 8. We show the results of a directly-modulated OIL (DM-OIL) laser in Fig. 8. The enhanced f_{RO} was 30 GHz. Note the drop in response starting close to dc, resulting in a 3-dB bandwidth of ~1 GHz, much lower than its resonance frequency. This is not due to the laser *RC* parasitics, as the 3-dB frequency of the *RC* parasitics is ~20 GHz.

For the MAM-OIL case, an EOM with a $f_{3\mathrm{dB}} = 25$ GHz was used for the modulation source. The resultant amplitude modulation output from the slave is shown in Fig. 8 (labeled MAM-OIL). Note the drop in the response near dc, as described in the previous section. As discussed before, the magnitude of the dip is reduced for more negative detuning frequencies. For the MPM-OIL case, a phase modulator with a $f_{3\mathrm{dB}} = 20$ GHz was use as the modulation source. The resultant phase modulation upon the slave is shown in Fig. 8 (labeled MPM-OIL). Note

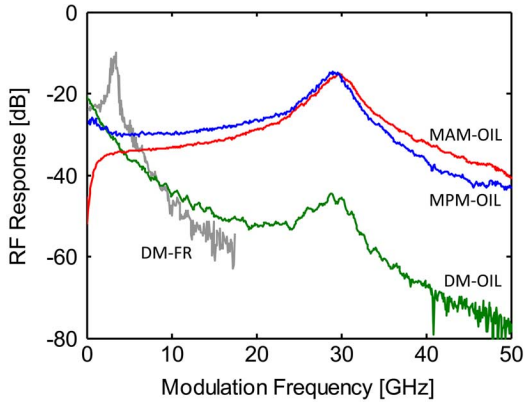

Fig. 8. Frequency response of an OIL laser under various modulation schemes. OIL conditions $(\Delta f, R)$ are held constant for all cases. DM-OIL: direct modulation of the OIL laser. MAM-OIL: Amplitude modulation of the injected light entering OIL laser. MPM-OIL: Phase modulation of the injected light entering OIL laser. DM-FR: Direct modulation of the free-running laser, shown for comparison. Modulator response was included in all curves.

that there is no dip at dc, and the response looks similar to that of a free-running, 2-pole laser (i.e., classic damped oscillator). The fitted resonance frequency for all OIL cases were found to be 30 GHz, and the fitted damping factors were all calculated to be within 3–4 GHz. This signifies that each OIL modulation scheme shares the same resonance and damping factor. However, the response between dc to resonance differs quite dramatically.

A. *Master Amplitude Modulation*

If we increase the injection locking parameters, we can optimize the enhanced EOM response. Fig. 9 shows the frequency response of the EOM, with a $f_{3\mathrm{dB}} = 25$ GHz. All response curves are normalized for cables, network analyzer, and photodetector response. The EOM exhibits a resonant notch at 55 GHz, possibly due to surface mode coupling or other effects. Note that this is not a fundamental limitation of the EOM. By injection locking the slave laser with the modulated light, we can tune the enhanced resonance of the OIL system to compensate for the notch, resulting in an enhanced $f_{3\mathrm{dB}} =$ 59 GHz [Fig. 9, line (a)]. The OIL conditions were $R = 8$ dB and $\Delta f = +27$ GHz. The tunability of the resonance can be used to create a broad resonance that can compensate for the typically slowly-decreasing response of an EOM, resulting in a flatter frequency response [Fig. 9, line (b)] ($R = 8.5$ dB and $\Delta f = +30$ GHz). We achieve a relatively flat response over > 70-GHz bandwidth, interrupted only by the 55-GHz resonant notch caused by the EOM itself. This is approaching the >3 times bandwidth enhancement limit predicted in the theory.

By tuning the detuning frequency, the resonance frequency can be tuned over a very wide range. Fig. 10 shows the normalized optical transmission response of the MAM-OIL laser, by subtracting the EOM response from the total response. Here, we changed Δf from 7 to 32 GHz, resulting in resonance frequencies of 73 to 107 GHz, respectively. Fig. 11 shows the experimental extraction of the resonance frequency across the entire locking map. Our experiments were limited to 110 GHz due to

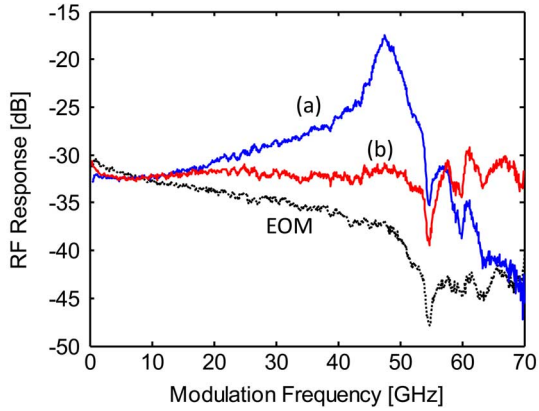

Fig. 9. Frequency response of EOM and two different bias conditions of MAM. (a) $\Delta f = 27$ GHz, $R = 8$ dB. (b) $\Delta f = 30$ GHz, $R = 8.5$ dB. (a) is optimized for 3-dB bandwidth ($f_{3\,\mathrm{dB}} = 59$ GHz) while (b) demonstrates $>$ 70-GHz flatness (aside from notch at 55 GHz).

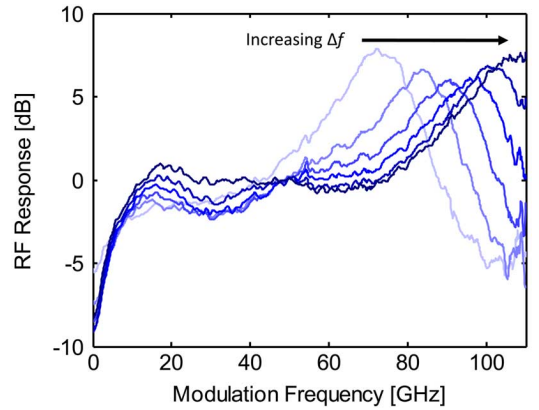

Fig. 10. Frequency response of MAM, after removing EOM response. $R = 8.6$ dB. The detuning frequency was tuned from 7 to 32 GHz, resulting in resonance frequencies from 73 to 107 GHz.

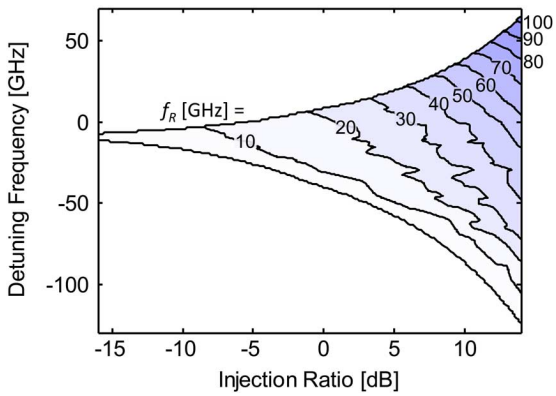

Fig. 11. Experimental plot of resonance frequency versus injection ratio and detuning frequency, across the stable locking range.

the network analyzer's maximum frequency limitation. However, the resonance frequency may be extended to well beyond 100 GHz.

The source of modulation is general, and any amplitude modulator can be used. In this case, we used an EOM. However,

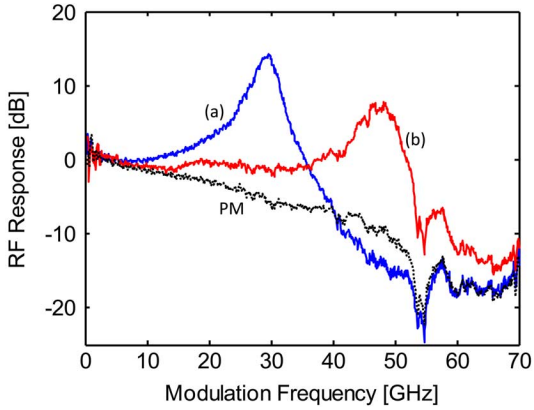

Fig. 12. Frequency response of PM and two different bias conditions of MPM. (a) $\Delta f = 12$ GHz, $R = 3$ dB. (b) $\Delta f = 25$ GHz, $R = 4$ dB. The bandwidths for the PM, (a), and (b) are 20, 36, and 53 GHz, respectively. The responses are not individually normalized to 0 dB, arid so they all exhibit the same magnitude DC response.

we have also performed amplitude modulation on an electroabsorption modulator laser [31] and direct-modulated, cascaded VCSELs [32].

B. Master Phase Modulation

We then performed similar experiments for the MPM-OIL configuration. Fig. 12 shows the frequency response of the MPM-OIL system for various injection conditions [Fig. 12, lines (a) and (b)]. As with all modulation schemes, including direct modulation, the resonance frequency increases with detuning frequency and injection ratio. The response of the 20-GHz PM is shown for reference [Fig. 12, line PM]. The noise at dc is an artifact of the AM/PM separation and detection technique. Since the actual detected value is proportional to the frequency modulation response, a factor of $1/f_m$ (where f_m is the modulation frequency) was applied to the signal to obtain the phase modulation response. The bandwidths of the PM, (a), and (b) are 20, 36, and 53 GHz, respectively. Hence, bandwidth enhancement can be obtained through this modulation scheme as in MAM-OIL. In addition, the MPM-OIL system does not exhibit the low-frequency suppression as in the case of MAM-OIL. As predicted in the theory [28], there is some amount of FM to AM conversion. However, with the proper choice of FM discrimination and detection system, this can be mitigated, or perhaps even beneficial.

IV. Conclusion

We have demonstrated optical amplitude and phase modulation of an injection-locked semiconductor laser. Both techniques are not limited by the low-frequency pole that dominates the bandwidth in the positive detuning frequency regime of directly-modulated OIL lasers. Furthermore, the slave laser's *RC* parasitics no longer limit the system's performance. Rather, we are relieved of the issues of engineering low laser parasitics and can focus our interest to the frequency performance of the modulation source. The benefit of the injection-locked laser is in providing an enhancement of bandwidth that can be dynamically tuned to different frequency bands. A maximum

three times enhancement of bandwidth can be shown theoretically, with experiment close to matching. Further bandwidth can be achieved by cascading injection-locked lasers [32]. The MAM-OIL technique is simple, requiring no coherent detection. However, in certain regimes, namely low injection ratios and positive detuning frequencies, it exhibits a low-frequency suppression. The MPM-OIL technique is more complex in detection. However, in the positive detuning frequency range, it does not exhibit a low-frequency suppression and exhibits a response resembling a classical laser with a tunable resonance frequency. We have demonstrated bandwidth enhancement up to 59 GHz for MAM-OIL and 53 GHz for MPM-OIL. These are enhancements of about 2.5 times the original bandwidth of the modulation source. We do expect noise and nonlinearities to increase at the resonance peak, depending on the magnitude of the peak. This will be addressed in a future paper. The technique of MAM-OIL and MPM-OIL has the potential to be used as an all-optical equalization technique for next-generation 100 Gb/s, as well as ultrahigh frequency RF applications.

ACKNOWLEDGMENT

The authors would like to thank Prof. R. Tucker of the University of Melbourne for helpful discussions.

REFERENCES

[1] R. S. Tucker, "High-speed modulation of semiconductor lasers," *J. Lightw. Technol.*, vol. 3, no. 6, pp. 1180–1192, Jun. 1985.

[2] Y. Matsui, H. Murai, S. Arahira, Y. Ogawa, and A. Suzuki, "Enhanced modulation bandwidth for strain-compensated InGaAlAs-InGaAsP MQW lasers," *IEEE J. Quantum Electron.*, vol. 34, no. 10, p. 1970, 1998.

[3] X. Zhang, A. Gutierrez-Aitken, D. Klotzkin, P. Bhattacharya, C. Caneau, and R. Bhat, "0.98-μm multiple-quantum-well tunneling injection laser with 98-GHz intrinsic modulation bandwidth," *IEEE J. Sel. Topics Quantum Electron.*, vol. 3, no. 2, pp. 309–14, 1997.

[4] S. Weisser, E. C. Larkins, K. Czotscher, W. Benz, J. Daleiden, I. Esquivias, J. Fleissner, J. D. Ralston, B. Romero, R. E. Sah, A. Schonfelder, and J. Rosenzweig, "Damping-limited modulation bandwidths up to 40 GHz in undoped short-cavity $In_{0.35}Ga_{0.65}As$–GaAs multiple-quantum-well lasers," *IEEE Photon. Technol. Lett.*, vol. 8, no. 5, pp. 608–10, 1996.

[5] K. Noguchi, O. Mitomi, and H. Miyazawa, "Millimeter-wave $Ti:LiNbO_3$ optical modulators," *J. Lightw. Technol.*, vol. 16, no. 4, pp. 615–19, Apr. 1998.

[6] R. Lewen, R. Lewen, S. Irmscher, U. Westergren, L. Thylen, and U. Eriksson, "Segmented transmission-line electroabsorption modulators," *J. Lightw. Technol.*, vol. 22, no. 1, pp. 172–179, Jan. 2004.

[7] T. B. Simpson and J. M. Liu, "Enhanced modulation bandwidth in injection-locked semiconductor lasers," *IEEE Photon. Technol. Lett.*, vol. 9, no. 10, pp. 1322–4, Oct. 1997.

[8] X. J. Meng, T. Chau, and M. C. Wu, "Experimental demonstration of modulation bandwidth enhancement in distributed feedback lasers with external light injection," *Electron. Lett.*, vol. 34, no. 21, p. 2031, Oct. 1998.

[9] L. Chrostowski, X. Zhao, and C. J. Chang-Hasnain, "Microwave performance of optically injection-locked VCSELs," *IEEE Trans. Microw. Theory Tech.*, vol. 54, no. 2, pp. 788–796, Feb. 2006.

[10] E. K. Lau, X. Zhao, H.-K. Sung, D. Parekh, C. Chang-Hasnain, and M. C. Wu, "Strong optical injection-locked semiconductor lasers demonstrating >100-GHz resonance frequencies and 80-GHz intrinsic bandwidths," *Opt. Express*, vol. 16, no. 9, pp. 6609–6618, 2008.

[11] E. K. Lau, H. K. Sung, and M. C. Wu, "Frequency response enhancement of optical injection-locked lasers," *IEEE J. Quantum Electron.*, vol. 44, no. 1, pp. 90–99, Jan. 2008.

[12] S. Wieczorek, W. W. Chow, L. Chrostowski, and C. J. Chang-Hasnain, "Improved semiconductor-laser dynamics from induced population pulsation," *IEEE J. Quantum Electron.*, vol. 42, no. 6, pp. 552–562, Jun. 2006.

[13] E. K. Lau, H.-K. Sung, X. Zhao, D. Parekh, C. J. Chang-Hasnain, and M. C. Wu, "Bandwidth enhancement by optical amplitude and phase modulation of injection-locked semiconductor lasers," in *Proc. Int. Topical Meeting Microw. Photon.*, Victoria, BC, Canada, 2007, pp. 241–244.

[14] M. K. Haldar, J. C. Coetzee, and K. B. Gan, "Optical frequency modulation and intensity modulation suppression in a master-slave semiconductor laser system with direct modulation of the master laser," *IEEE J. Quantum Electron.*, vol. 41, no. 3, pp. 280–6, Mar. 2005.

[15] S. Kasapi, S. Lathi, and Y. Yamamoto, "Sub-shot-noise frequency-modulation spectroscopy by use of amplitude-squeezed light from semiconductor lasers," *J. Opt. Soc. Amer. B*, vol. 17, no. 2, pp. 275–9, 2000.

[16] E. Wong, X. Zhao, C. J. Chang-Hasnain, W. Hofmann, and M. C. Amann, "Optically injection-locked 1.55-μm VCSELs as upstream transmitters in WDM-PONs," *IEEE Photon. Technol. Lett.*, vol. 18, no. 22, pp. 2371–3, Nov. 2006.

[17] M. Bhattacharya and T. Chatlopadhyay, "A method for generation of optical FM signal through injection locking," *J. Lightw. Technol.*, vol. 16, no. 4, pp. 656–660, Apr. 1998.

[18] S. Kobayashi and T. Kimura, "Optical FM signal amplification by injection locked and resonant type semiconductor laser amplifiers," *IEEE J. Quantum Electron.*, vol. 18, no. 4, p. 575, Apr. 1982.

[19] L. Li, "Small signal analysis of optical FM signal amplification by an injection-locked type semiconductor laser amplifier," *J. Lightw. Technol.*, vol. 10, no. 4, pp. 477–481, Apr. 1992.

[20] P. Spano, M. Tamburrini, and S. Piazzolla, "Optical FSK modulation using injection-locked laser diodes," *J. Lightw. Technol.*, vol. 7, no. 4, pp. 726–728, Apr. 1989.

[21] M. Vainio, M. Merimaa, and K. Nyholm, "Modulation transfer characteristics of injection-locked diode lasers," *Opt. Commun.*, vol. 267, no. 2, pp. 455–463, 2006.

[22] H. Nakajima, R. Derouiche, J. Charil, and P. Correc, "Reception of frequency-modulated optical signals through intracavity optical power change in injection-locked $\lambda/4$-shifted DFB laser," *Electron. Lett.*, vol. 28, no. 14, pp. 1342–4, 1992.

[23] H. Shimizu, H. Shimizu, and Y. Nakano, "Monolithic integration of a waveguide optical isolator with a distributed feedback laser diode in the 1.5-μm wavelength range," *IEEE Photon. Technol. Lett.*, vol. 19, no. 24, pp. 1973–1975, Dec. 2007.

[24] F. Mogensen, H. Olesen, and G. Jacobsen, "Locking conditions and stability properties for a semiconductor laser with external light injection," *IEEE J. Quantum Electron.*, vol. QE-21, no. 7, pp. 784–93, Jul. 1985.

[25] C. H. Henry, N. A. Olsson, and N. K. Dutta, "Locking range and stability of injection locked 1.54 μm InGaAsP semiconductor lasers," *IEEE J. Quantum Electron.*, vol. QE-21, no. 8, pp. 1152–6, Aug. 1985.

[26] R. Lang, "Injection locking properties of a semiconductor laser," *IEEE J. Quantum Electron.*, vol. QE-18, no. 6, pp. 976–83, Jun. 1982.

[27] A. Murakami, K. Kawashima, and K. Atsuki, "Cavity resonance shift and bandwidth enhancement in semiconductor lasers with strong light injection," *IEEE J. Quantum Electron.*, vol. 39, no. 10, pp. 1196–204, Oct. 2003.

[28] E. K. Lau and M. C. Wu, "Amplitude and frequency modulation of the master laser in injection-locked laser systems," in *Proc. Int. Topical Meeting Microw. Photon.*, Ogunquit, ME, 2004, pp. 142–5.

[29] E. K. Lau, H. K. Sung, and M. C. Wu, "Scaling of resonance frequency for strong injection-locked lasers," *Opt. Lett.*, vol. 32, no. 23, pp. 3373–3375, 2007.

[30] W. V. Sorin, K. W. Chang, G. A. Conrad, and P. R. Hernday, "Frequency domain analysis of an optical FM discriminator," *J. Lightw. Technol.*, vol. 10, no. 6, pp. 787–93, Jun. 1992.

[31] E. K. Lau, H. K. Sung, X. Zhao, D. Parekh, C. J. Chang-Hasnain, and M. C. Wu, "Bandwidth enhancement of electro-absorption modulated lasers by optical injection locking," in *Proc. Annu. Meeting IEEE Lasers and Electro-Optics Soc.*, Lake Buena Vista, FL, 2007, pp. 188–189.

[32] X. Zhao, D. Parekh, E. K. Lau, H. K. Sung, M. C. Wu, and C. J. Chang-Hasnain, "Novel cascaded injection-locked 1.55-μm VCSELs with 66 GHz modulation bandwidth," *Opt. Express*, vol. 15, no. 22, pp. 14810–14816, 2007.

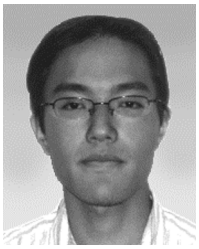

Erwin K. Lau (S'01–M'06) received the B.S. and M.Eng. degrees in electrical engineering from the Massachusetts Institute of Technology, Cambridge, in 2000 and 2001, respectively and the Ph.D. degree in electrical engineering and computer sciences from the University of California, Berkeley, in 2006.

In 2004, he spent a summer at the IBM Thomas J. Watson Research Center, Yorktown, NY, where he worked on noise of parallel digital optical interconnects. He is currently a Postdoctoral Researcher in electrical engineering at the University of California, Berkeley. His research interests are on optical injection locking of semiconductor lasers and high-speed optical communications.

Dr. Lau is a member of the Optical Society of America (OSA). He is a 2002–2003 Hertz Fellowship Finalist.

Liang Jie Wong is currently working towards the B.S. degree in electrical engineering and computer sciences at the University of California, Berkeley.

He is a National Science Scholar of the Agency of Science, Technology and Research, Singapore, and a Regents' and Chancellor's Scholar of the University of California, Berkeley. His research interests include high-speed RF photonics and semiconductor laser noise.

Xiaoxue Zhao (M'08) received the B.S. degree in electronics from Peking University, Beijing, China, in 2003. She is currently working towards the Ph.D. degree in electrical engineering and computer sciences at the University of California, Berkeley.

Her research interests are in microwave photonics, high-speed modulation of vertical-cavity surface-emitting lasers, optical injection locking, and optical communication systems.

Young-Kai Chen (S'78–M'86–SM'94–F'98) received the B.S.E.E. degree from National Chiao Tung University, Taiwan, R.O.C., the M.S.E.E. degree from Syracuse University, Syracuse, NY, and the Ph.D. degree from Cornell University, Ithaca, NY, in 1988.

From 1980 to 1985, he was a Member of Technical Staff in the Electronics Laboratory of General Electric Company, Syracuse, NY, where he was responsible for the design of silicon and GaAs MMICs for phase array applications. Since February 1988, he has been with Bell Laboratories, Murray Hill, NJ, as a Member of Technical Staff. Since 1994, he was the Director of High Speed Electronics Research. He is currently the Director of the High Speed Electronics and Optoelectronics Research Department, Bell Laboratories, Alcatel-Lucent. He is also an Adjunct Associated Professor at Columbia University, New York. His research interest is in high-speed semiconductor devices and circuits for wireless and optic fiber communications. He has contributed to more than 100 technical papers and 15 patents in the field of high-frequency electronic devices, circuits and semiconductor lasers.

Dr. Chen is a Bell Labs Fellow and a member of the National Academy of Engineering. He is the recipient of the 2002 IEEE David Sarnoff Award.

Connie J. Chang-Hasnain (M'88–SM'92–F'98) received the B.S. degree from the University of California, Davis, in 1982 and the M.S. and Ph.D. degrees from the University of California, Berkeley, in 1984, and 1987, respectively, all in electrical engineering.

She was a Member of Technical Staff at Bellcore from 1987 to 1992. From April 1992 to December 1995, she was an Associate Professor of electrical engineering at Stanford University, Stanford, CA. Since January 1996, she has been a Professor in the Department of Electrical Engineering, University of California, Berkeley. Since 2004, she has been Director of the Center for Optoelectronic Nanostructured Semiconductor Technologies (CONSRT). Her research interests are in nanostructured materials, nano- and micro- optoelectronic devices, and their applications. She coauthored 283 research papers in technical journals and conferences and six book chapters. She also has 26 patents granted.

Prof. Chang-Hasnain was named a Presidential Faculty Fellow, a National Young Investigator, a Packard Fellow, a Sloan Research Fellow, and Outstanding Young Electrical Engineer of the Year by Eta Kappa Nu. She received the 1994 IEEE LEOS Distinguished Lecturer Award, the 2000 Curtis W. McGraw Research Award from the American Society of Engineering Education, the 2003 IEEE William Streifer Scientific Achievement Award, and the 2005 Gilbreth Lecturer Award from the National Academy of Engineering. She is a Fellow of the Optical Society of America (OSA) and Institution of Electrical Engineers (IEE), and an Associate Editor for the JOURNAL OF LIGHTWAVE TECHNOLOGY. She was elected an Honorary Member of A.F. Ioffe Institute in 2005.

Ming C. Wu (S'82–M'83–SM'00–F'02) received the M.S. and Ph.D. degrees in electrical engineering from the University of California, Berkeley, in 1985 and 1988, respectively.

From 1988 to 1992, he was a Member of Technical Staff at AT&T Bell Laboratories, Murray Hill, NJ. From 1992 to 2004, he was a Professor in the Electrical Engineering Department at the University of California, Los Angeles. In 2004, he joined the University of California, Berkeley, where he is currently Professor of Electrical Engineering and Computer Sciences and Co-Director of Berkeley Sensor and Actuator Center (BSAC). His research interests include micro- and nanoelectromechanical systems (MEMS/NEMS), optofluidics, optoelectronics, nanophotonics, and biophotonics. He has published six book chapters, 140 journal and 300 conference papers, and holds 16 U.S. patents.

Prof. Wu is a member of Optical Society of America (OSA). He was a Packard Foundation Fellow from 1992 to 1997, and received the 2007 Engineering Excellence Award from the OSA.